Improved representation of isoprene-derived secondary organic aerosol in CAM6-Chem reveals regional contrasts in its long-term changes over China

Wenxin Zhang[1], Man Yue[1,2], Xinyue Shao[1], Xinyi Dong[1,3,4], Minghuai Wang[1,4]

[1]School of Atmospheric Science, Nanjing University, Nanjing, 210023, China
[2]Zhejiang Institute of Meteorological Sciences, Hangzhou, 310008, China
[3]Frontiers Science Center for Critical Earth Material Cycling, Nanjing University
[4]Joint International Research Laboratory of Atmospheric and Earth System Sciences & Institute for Climate and Global Change Research, Nanjing University, Nanjing, 210023, China

Correspondence to: Xinyi Dong (dongxy@nju.edu.cn)

Text S1: Multiple regression supplement. The standardized regression analysis was based on regional-mean monthly time series derived by spatially averaging the original monthly gridded data for each variable over Southwest China (SWC) and the Shaanxi–Gansu–Ningxia region (SGN). The mean seasonal cycle was then removed from each time series to obtain monthly anomalies, followed by z-score standardization so that all variables had zero mean and unit variance and could be compared on a common scale. Multiple linear regression was subsequently applied to the standardized anomalies, and the resulting standardized regression coefficients (β) were used to quantify the relative importance of individual predictors. To further compare their contributions, we calculated the normalized importance of each factor as $|\beta|/\Sigma|\beta|$. Because this analysis is based on deseasonalized monthly anomalies, the standardized β values primarily reflect the dominant drivers of regional month-to-month isoprene-derived secondary organic aerosol (ISOA) variability (Table S1). The regression results show that biogenic isoprene emissions are the most important predictor of monthly ISOA variability in both regions. In SWC, isoprene emissions have the largest standardized coefficient ($\beta = 0.45$, $p < 0.001$) and account for 49.937% of the total explained relative importance (Table S1), indicating that isoprene precursor supply dominates short-term ISOA variability in this region. Sulfate is the second-largest contributor ($\beta = 0.23$, 25.491%), whereas the contributions of anthropogenic nitrogen oxides (NOx) emissions, aerosol liquid water, and log10(H^+) are smaller (Table S1). In SGN, isoprene emissions also have the largest standardized coefficient ($\beta = 0.45$, $p < 0.001$) and the highest relative importance (32.312%), but sulfate shows a comparable contribution ($\beta = 0.39$, 28.319%), suggesting a stronger role of the heterogeneous reaction medium in modulating ISOA variability there (Table S1). Anthropogenic NOx emissions and log10(H+) show moderate contributions in SGN, whereas aerosol liquid water remains relatively weak (Table S1). Overall, the regression analysis indicates that month-to-month ISOA variability in SWC is primarily controlled by biogenic precursor supply, while variability in SGN reflects a more balanced influence of precursor supply and sulfate-related heterogeneous processing.

Driver	SWC					SGN				
	r	p_r	β	p_β	Importance (%)	r	p_r	β	p_β	Importance (%)
ISOP emis	0.49	<0.001	0.45	<0.001	**49.94**	0.45	<0.001	**0.45**	<0.001	**32.31**
SO_4^{2-}	0.41	0.001	0.23	0.234	25.49	0.34	0.009	0.39	0.130	28.32
Anthro NOx emis	0.37	0.004	0.12	0.401	13.30	-0.16	0.221	-0.23	0.090	16.36
AeroWater	0.37	0.004	0.10	0.664	10.59	0.21	0.117	-0.140	0.674	10.00
log10(H^+)	0.33	0.010	-0.01	0.972	0.69	0.26	0.049	0.18	0.359	13.02

Table S1: Standardized multiple linear regression results for monthly isoprene-derived secondary organic aerosol (ISOA) variability in Southwest China (SWC) and the Shaanxi–Gansu–Ningxia region (SGN). The regression is based on deseasonalized monthly anomalies that were subsequently z-score standardized, using data from the five simulation years (2000, 2006, 2012, 2016, and 2019). For each driver, the table lists the pearson correlation coefficient (r), significance level (p_r), standardized regression coefficient (β), significance level (p_β), and normalized relative importance (|β|/Σ|β|; %). Bold values indicate the largest normalized relative importance in each region.

Text S2. Region-specific temporal evolution of major ISOA sub-species in SWC and SGN. Based on the analyses in Section. 3.3, we further examined the temporal evolution of the four major ISOA subspecies in SWC and SGN to provide additional process-based interpretation of the contrasting regional ISOA trends. In both regions, paired subspecies within each pathway exhibit highly coherent temporal variations, indicating that their evolution is governed by common pathway-specific controls. However, the peak timing and subsequent evolution of these subspecies differ markedly between SWC and SGN, suggesting that the mechanisms controlling ISOA changes are region-dependent.

In SWC, the temporal evolution of the four major ISOA subspecies shows a clear separation in peak years between the low-NOx and high-NOx pathways (Fig. 8(a)). AIETET and AIEOSN, which are formed through the low-NOx pathway, both peak in 2006 and then decline thereafter, whereas AHMGA and AHMOSN, which are associated with the high-NOx pathway, reach their maxima later, in 2012. This divergence in peak timing reflects the different sensitivities of the two pathways to precursor supply and reaction-medium conditions. After 2006, decreasing anthropogenic sulfur dioxide (SO_2) emissions led to a decline in sulfate (Fig. 8(b,d)), thereby weakening the heterogeneous reaction medium required by the low-NOx pathway. As a result, although biogenic isoprene emissions continue to increase and precursor concentrations remain elevated during this period (Fig. 8(b,c)), these favorable changes in precursor supply are insufficient to offset the weakening of the sulfate-related reaction medium, causing AIETET and AIEOSN to shift from their 2006 maxima into a sustained decline. In contrast, the high-NOx pathway exhibits a different response. HMML and MAE are characteristic gas-phase precursors of the high-NOx pathway,

and their formation is more sensitive to changes in anthropogenic NOx emissions. Because NOx emissions continue to rise and reach a maximum in 2012 (Fig. 8(b)), precursor supply for ISOA formed through the HMML + MAE pathway is sustained for a longer period. In addition, although sulfate decreases after 2006, aerosol liquid water remains at a relatively high level and reaches a maximum in 2012 (Fig. 8(d)), providing an alternative reaction medium for the heterogeneous uptake of HMML and MAE and partly compensating for the adverse effect of sulfate reduction. Therefore, in SWC, products from the low-NOx pathway are more sensitive to sulfate-related reaction-medium conditions, whereas products from the high-NOx pathway depend more strongly on precursor supply. This interpretation is also broadly consistent with the trend attribution results in Table 2, which indicate that biogenic isoprene emissions, anthropogenic NOx emissions, and sulfate all play important roles in shaping ISOA changes in SWC, although biogenic isoprene emissions make the largest contribution. In SGN, products from both the low-NOx and high-NOx pathways peak in 2006 and decline thereafter (Fig. 8(a)), indicating that their temporal evolution is more uniformly constrained than in SWC. The low-NOx products more closely follow the post-2006 sulfate decline, suggesting a stronger dependence on sulfate-related heterogeneous processing. By contrast, although NOx emissions and HMML + MAE continue to increase until 2012, the high-NOx products still show an overall decline, indicating that enhanced precursor supply cannot compensate for the weakening of the reaction medium. The smaller decline in the high-NOx products nevertheless suggests that rising NOx emissions partly mitigate this unfavorable effect. This interpretation is also consistent with the trend attribution results in Table 1, which identify sulfate and anthropogenic NOx emissions as the two leading contributors to ISOA changes in SGN.

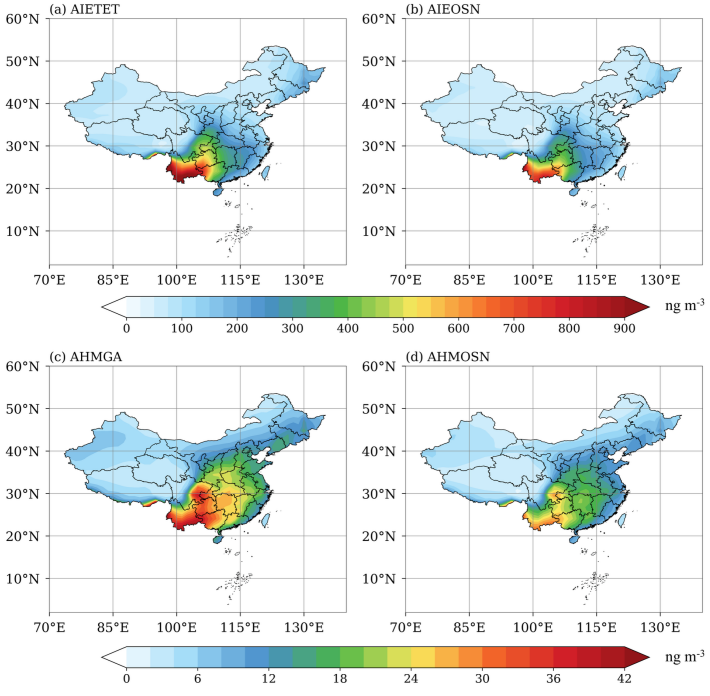

Figure S1: Mean annual surface concentrations of four isoprene-derived secondary organic aerosol (ISOA) subspecies (AIETET, AIEOSN, AHMGA, and AHMOSN) in China from 2000 to 2019 (unit: ng m^{-3}).

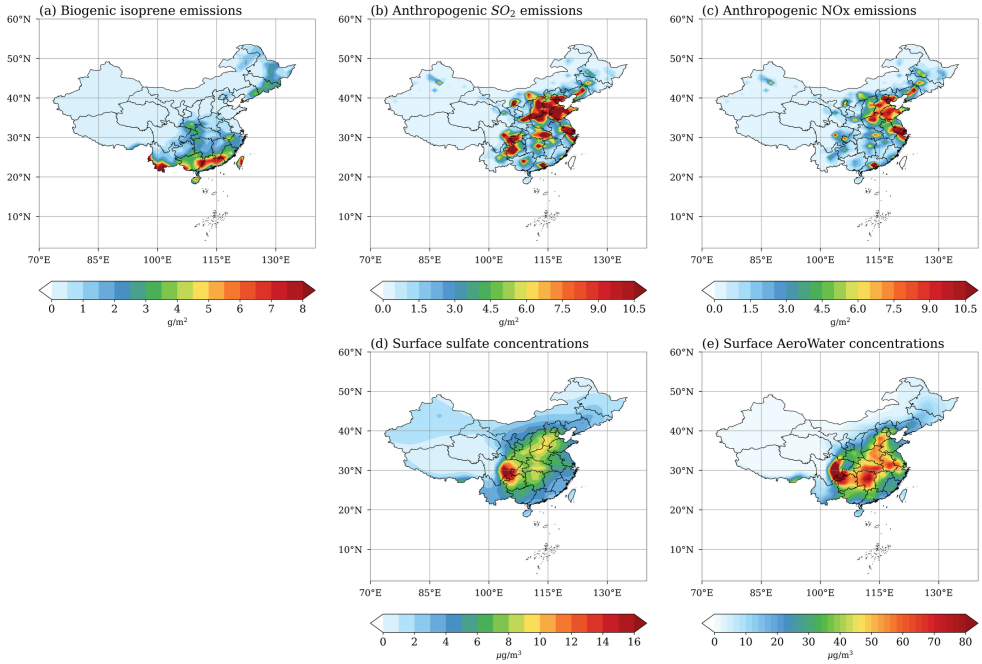

Figure S2: Mean annual biogenic isoprene emissions (a; unit: g m^{-2}), anthropogenic sulfur dioxide (SO_2) emissions (b; unit: g m^{-2}), anthropogenic nitrogen oxides (NOx) emissions (c; unit: g m^{-2}), surface sulfate concentrations (d; μg m^{-3}), and surface aerosol liquid water (AeroWater) concentrations (e; μg m^{-3}), in China from 2000 to 2019.

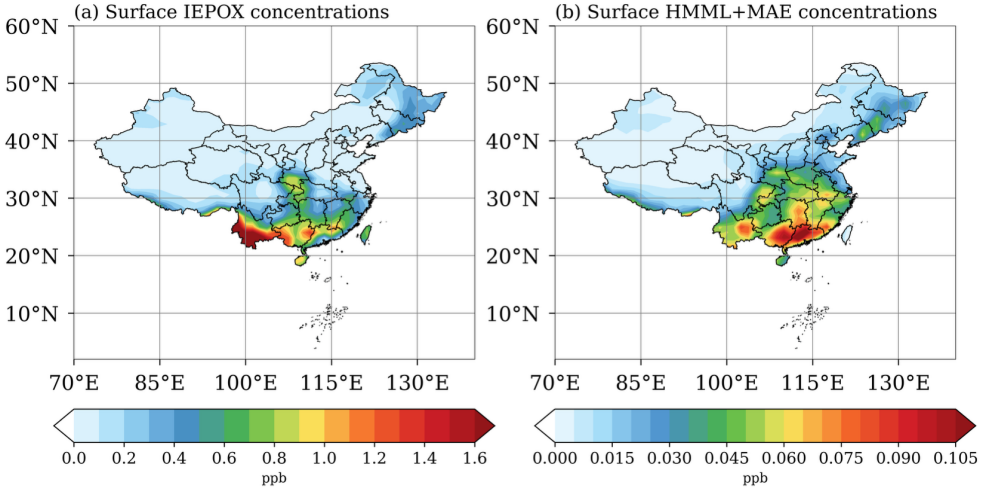

Figure S3: Mean annual surface isoprene epoxydiols (IEPOX) concentrations (a; unit: ppb) and surface hydroxymethyl-methyl-α-lactone plus methacrylic acid epoxide (HMML + MAE) concentrations (b; unit: ppb), in China from 2000 to 2019.

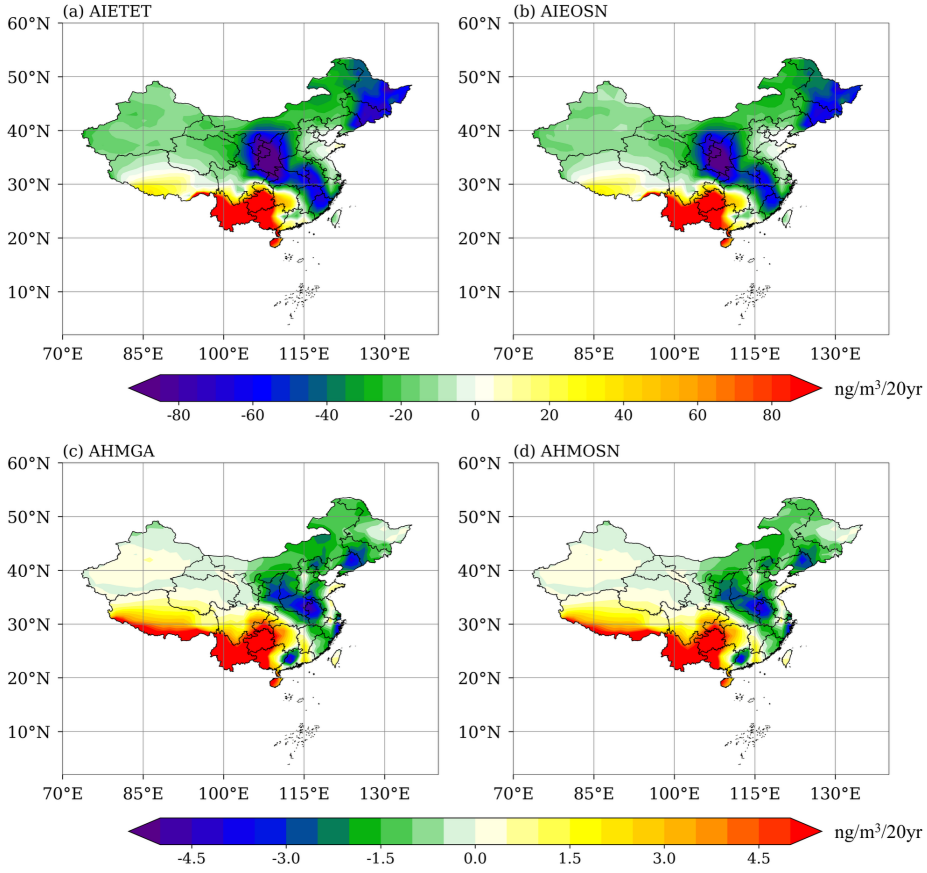

Figure S4: Annual average long-term trends of four isoprene-derived secondary organic aerosol (ISOA) subspecies (AIETET, AIEOSN, AHMGA, and AHMOSN) surface concentrations (ng m^{-3} per 20 years), in China from 2000 to 2019.

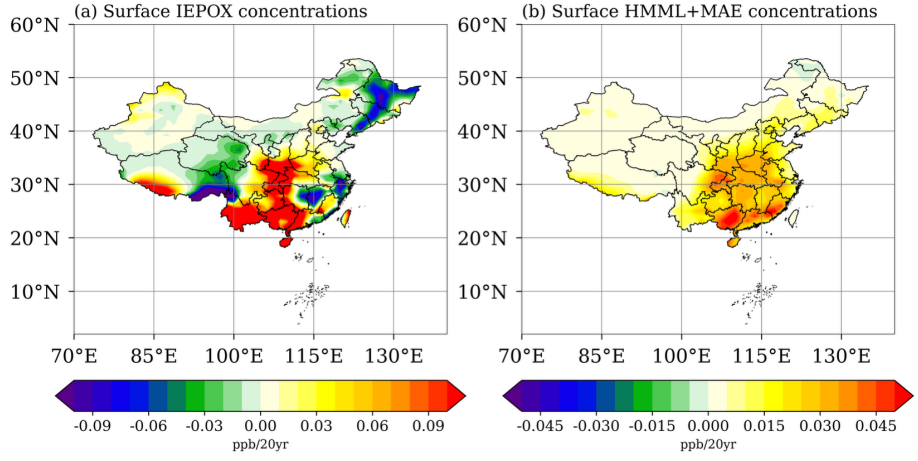

Figure S5: Annual average long-term trends of (a) surface isoprene epoxydiols (IEPOX) concentrations and (b) surface hydroxymethyl-methyl-α-lactone plus methacrylic acid epoxide (HMML + MAE) concentrations (ppb per 20 years), in China from 2000 to 2019.

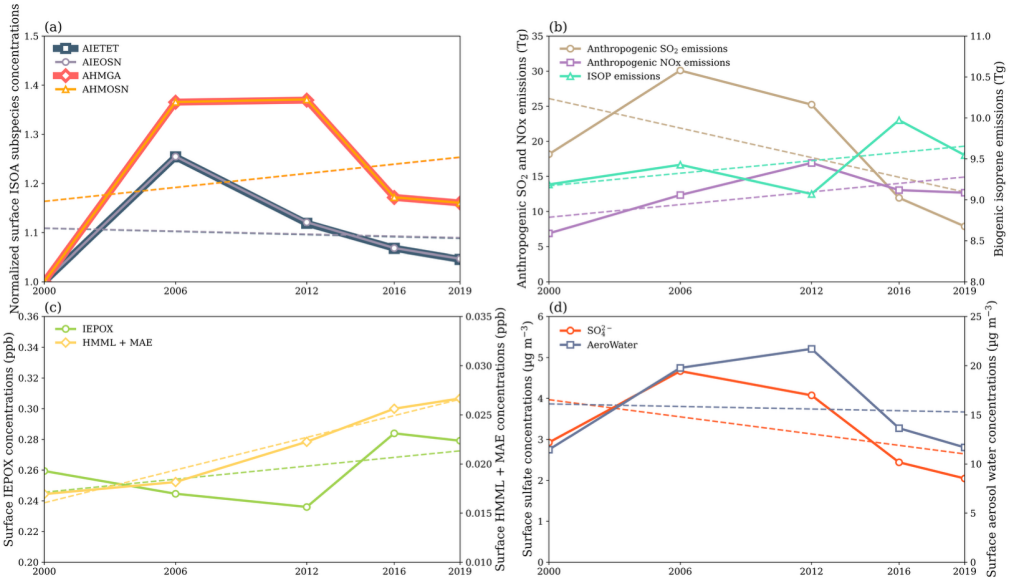

Figure S6: Time series of (a) normalized surface isoprene-derived secondary organic aerosol (ISOA) subspecies concentrations (the normalized values are calculated as the ratio of the value in each year to that in 2000); (b) anthropogenic sulfur dioxide (SO_2) emissions and anthropogenic nitrogen oxides (NOx) emissions (left y axis; unit: Tg), and biogenic isoprene emissions (right y axis; unit: Tg); (c) surface isoprene epoxydiols (IEPOX) concentrations (left y axis; unit: ppb) and surface hydroxymethyl-methyl-α-lactone plus methacrylic acid epoxide (HMML + MAE) concentrations (right y axis; unit: ppb); and (d) surface sulfate (SO_4^{2-}) concentrations (left y axis; unit: μg m^{-3}) and surface aerosol liquid water (AeroWater) concentrations (right y axis; unit: μg m^{-3}) in China.

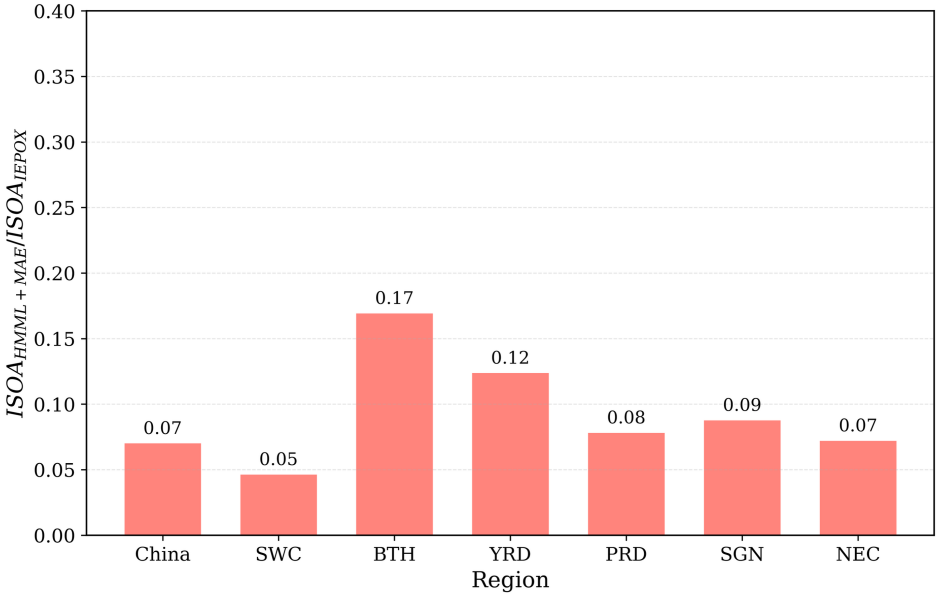

Figure S7: Ratios of multi-year mean surface concentrations of ISOA derived from HMML and MAE ($ISOA_{HMML+MAE}$) to those derived from IEPOX ($ISOA_{IEPOX}$) in China and selected subregions from 2000 to 2019, including Southwest China (SWC), the Beijing–Tianjin–Hebei region (BTH), the Yangtze River Delta (YRD), the Pearl River Delta (PRD), the Shaanxi–Gansu–Ningxia region (SGN), and Northeast China (NEC).

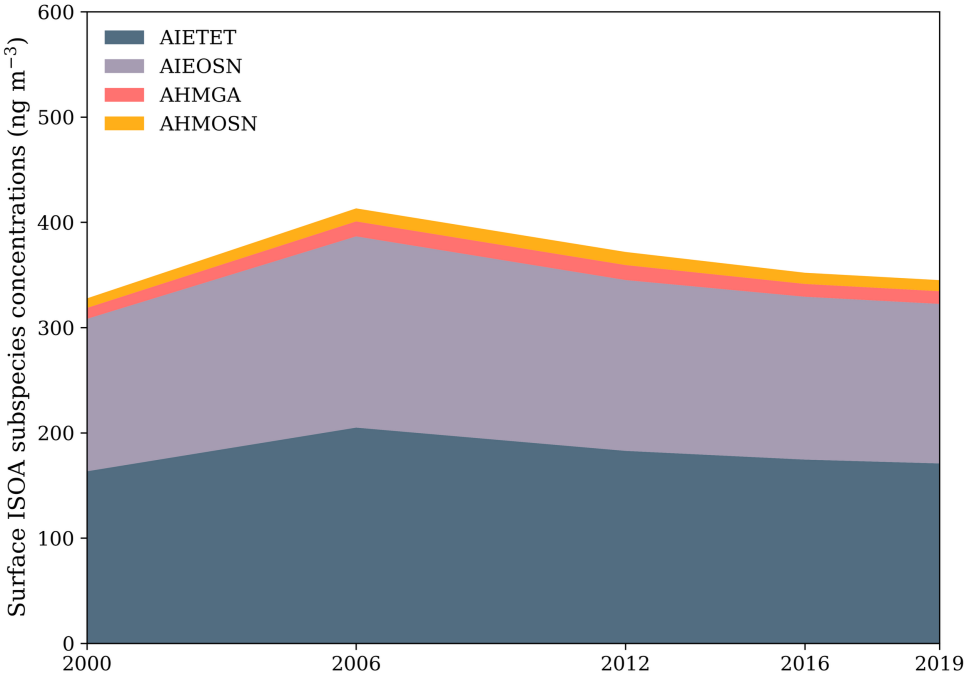

Figure S8: Interannual variations of average surface isoprene-derived secondary organic aerosol (ISOA) subspecies concentrations from 2000 to 2019 (unit: ng m^{-3}).

Equation	Rate coefficient/parameters
MACR + NO2 -> MPAN	9.7e-29, 5.6, 9.3e-12, 1.5, 0.6
MPAN + OH -> 0.03*CO + 0.81*NO_3 + 0.21*MAE + 0.57*HMML + 0.19*PAN + 0.19*HO_2	3.00e-11

Table S2: Newly added gas-phase reactions for the updated high-NOx isoprene chemistry and their rate constants in this study. For the first reaction, the listed five parameters follow the standard CESM/MOZART falloff formulation and represent the low-pressure-limit pre-exponential factor, its temperature exponent, the high-pressure-limit pre-exponential factor, its temperature exponent, and the broadening factor, respectively. For the second reaction, the listed value is the temperature-independent Arrhenius rate constant.